



Exploration of effect of delignification on the mesopore structure in poplar cell wall by nitrogen absorption method

Rui Liang · Yu-Hui Zhu · Liang Wen · Wan-Wan Zhao · Bing-Bin Kuai · Yao-Li Zhang · Li-Ping Cai

Received: 10 June 2019 / Accepted: 7 December 2019 / Published online: 21 December 2019
© Springer Nature B.V. 2019

Abstract As an important commodity wood material, poplar has porous structure, which is worthy of being investigated. Especially, the lignin concentration is closely related to the formation and change of pores. Although a few studies reported the relation between the pore volume and the lignin removal of the ground wood (Stone and Scallan in *J Polym Sci C Polym Symp* 11(1):13–25, 1965), no information of the distribution of pore sizes versus the whole delignification process steps was reported. This study initially explored the effect of delignification level on the pore size distribution and pore structure in poplar cell walls using nitrogen absorption measurement. It was found that delignification increased the N₂ adsorption amount and specific surface area of poplar. It also caused a large number of mesopores in the cell wall, mainly in the 2–10 nm pore size range, and decreased the average pore size. The whole delignification process can be roughly divided into three major phases, namely, the initial phase, the transitional phase and the stable phase, in which, the change

process was not completely uniform. During the delignification, the size of poplar cell wall pores continued reducing, and finally a large number of uniform pores of about 2.1 nm was formed.

Keywords BJH method · N₂ adsorption method · Poplar · Mesopore structure · Pore diameter distribution · Pore volume · Progressive delignification

Introduction

Porosity is one of the most important features of cellulosic material, which affects its properties and utilization prospect (Meng et al. 2013). As one of the cellulosic materials, wood has not only macroscopic pores, but also pores with specific multi-scale pore structure of macroscopic–mesoscopic–microscopic systems (Ruelle 2014; Sarkar and Auer 2017). The porosity of wood, especially microscopic pores, is an important indicator of the wood properties. The microscopic and mesoscopic pores of wood have a great influence on the performances of the water movement, heat transfer in wood and the permeability of wood. In general, pores were classified according to micropores (< 2 nm), mesopores (2–50 nm), and macropores (> 50 nm) (Barrett et al. 1951). The studies of wood pores have evolved from macroscopic to nanoscale, mainly for the distribution and variation

R. Liang · Y.-H. Zhu · L. Wen · W.-W. Zhao · B.-B. Kuai · Y.-L. Zhang (✉) · L.-P. Cai
College of Material Science and Engineering, Nanjing Forestry University, Nanjing 210037, People's Republic of China
e-mail: zhangyaoli@126.com

L.-P. Cai
Department of Mechanical and Energy Engineering,
University of North Texas, Denton, TX 76203, USA

of micropores and mesopores (Stone 1964; Akitomo et al. 2006).

At present, the examination of microscopic pores in wood cell walls cannot be directly observed by the electron microscopy (Fahlén and Salmén 2005). Therefore, gas adsorption is often used to obtain the pore data. Generally, CO₂ and N₂ are often used as adsorption media for the measuring of micropores and mesopores, respectively (Nakatani et al. 2008; Kojiro et al. 2010). The N₂ adsorption method is a physical adsorption type that can be used for a single layer and multilayer adsorptions (Brunauer et al. 1938). This method is highly accurate in the determination of the characteristics of porous materials, and many calculation models can be applied to pores measuring in different states (Galarnau et al. 1999; He et al. 2004; Rouquerol et al. 2013). The pores of the wood cell wall are generally considered to be slit-like or directly simplified into a cylindrical shape. The two models of pore morphology, Innes and BJH (Barrett–Joiner–Halenda) methods, can be found to be similar in their results, so the BJH model is commonly used for mesoporosity analysis of wood (Innes 1957; Kimura et al. 2016).

Porosity in the wood cell wall helps to analyze the maturity of the tension wood, especially in the structural correlation of the G-layer. Tension wood is a special type of wood, in which the source and mechanism of tension are of concern. The introduction of the mesoporosity concept supported the hypothesis of G-layer matrix swelling during maturation (Chang et al. 2009, 2011a, 2015).

Wood chemical treatment and carbonization lead to changes in the pore structure of the wood cell wall, mainly during the heat treatment, the high temperature makes the pores closed, so the dried wood has much less pores than the wet one (Kojiro et al. 2008, 2010). Moreover, the reduction number of micropores is larger than that of mesopores, and this phenomenon can be reproduced by wetting and drying (Borrega and Kärenlampi 2011). However, the pore volume increases as the temperature rises to thermal degradation (Monteiro 2018).

The formation of wood pores is strongly related to the chemical composition. Many studies pointed out that lignin and cell wall pores are inextricably linked (Yin et al. 2015; Shi and Avramidis 2018). Moreover, the difference in pore structure between heartwood and sapwood, softwood and hardwood, also validated

this theory (Donaldson et al. 2018). Lignin was associated with micropores smaller than 0.6 nm, so delignification reduced micropores and increased mesopores (Stone and Scallan 1965; Nakatani et al. 2008; Kojiro et al. 2010).

There are many applications related to lignin in the processing and utilization of wood, such as paper pulping, production of activated carbon, silicification of wood, preparation of transparent wood, biological conversion of biomass, etc. The studies on the pore distribution of pulp have been always reported. A large amount of lignin is removed and a large number of mesopores is created during the pulping process (Stone and Scallan 1965; Kimura et al. 2014). Lignin is also a useful biological resource for the production of activated carbon. The higher lignin content can make the activated carbon that has larger micropore specific surface area with ability to effectively adsorb metal impurities in water (Dizhbite et al. 1999; Basso et al. 2005; Carrott and Carrott 2007). In addition to this, some new materials are involved in the preparation of delignification. On the one hand, silicification of wood can be used to preserve fossil wood to help examine the microstructure of wood (Persson et al. 2004a, b; Dietrich et al. 2013); on the other hand, wood template can be used to make advanced ceramic materials (Mizutani et al. 2005; Deshpande et al. 2006; Dietrich et al. 2015). The process of making wood template from delignification was also used in the preparation of transparent wood. Transparent wood not only breaks through the traditional appearance of wood, but also has great promise in terms of optical properties, architectural applications, and the addition of particles for special performance (Fink 1992; Zhu et al. 2016; Wang et al. 2018b; Wu et al. 2019). Pretreatment not only affected the surface area and pore distribution, but also controlled cellulase access to cellulose. The accessibility of enzymes is an important factor in the conversion of biomass (Ishizawa et al. 2007; Meng et al. 2013, 2015).

Therefore, the relation between lignin and the pore structure in wood cell wall is crucial. Furthermore, lignin is one of the three major chemical components of wood, and its existence and corresponding pore change laws are worthy of being further investigated. However, in terms of pore structure, there were more studies on softwoods while less on hardwoods. Interest has recently arisen in the delignification of wood, driven by the development of functional wood

products (e.g. paper pulping and transparent wood), which needs to be pre-treated by delignification. However, the studies regarding the relationship between delignification process and the pore structure of wood were limited. Although a few studies reported the relation between the pore volume and the lignin removal of the ground wood (Stone and Scallan 1965), no information of the distribution of pore sizes versus the whole delignification process steps was reported. This study initially explored the effect of delignification level on the pore size distribution and pore structure in poplar cell walls using nitrogen absorption measurement, which is of great significance for expanding the application range of fast-growing poplar.

Materials and methods

Materials

The samples were hybrid poplar clones collected from the Jiaozuo forest farm in Henan Province, China. The tree height was 18.8 m, the breast diameter was 22.4 cm, and the tree age was 10 years. A two-meter-long section from 3.5 to 5.5 m along the longitudinal direction of the tree was taken. The experimental samples were cut from the fourth annual ring near the bark (sapwood). A plurality of sections was continuously taken along one end of the trunk and air-dried under the laboratory atmospheric condition. After the drying, a sufficient amount of material in fourth annual ring was cut. In order to carry out the delignification and nitrogen adsorption experiments, the wood blocks were cut into small strips with a cross section of about 2×2 mm.

Delignification

The small wooden strips were divided into five groups, 15–20 g each. For the progressive delignification treatment, it was expected the gradient interval of about 25%, which means five groups would be removed about 0%, 25%, 50%, 75%, and 95% lignin, respectively. The delignification treatment used a dissociation solution of 1:1 configuration of 30% hydrogen peroxide and glacial acetic acid (Franklin 1945). The five groups of wood strips were completely immersed in the dissociation agent and placed in a

constant temperature water bath at 40 °C for reaction of 0 h, 1 h, 6 h, 10 h or 32 h, respectively. After the reaction, the fiber samples were rinsed by deionized water. During the 48-h rinsing process, the deionized water was changed every 8 h to remove the components of the dissociation, hydrogen peroxide and glacial acetic acid. To avoid damaging the cell wall structures, samples were then dried at 65 ± 2 °C in an oven because 65 °C is a relatively low temperature for drying. Under this condition, generally, the components of wood cell wall would not be degraded, so the pore structure could be protected (Dawson and Pearson 2017). During the progressive delignification process, middle lamellas of samples were not totally separated. In this way, pores could be produced in middle lamellas. However, generally speaking, the middle lamella is also a part of the structure of the wood cell walls; therefore, pores of poplar included the pores of the middle lamellas after the delignification.

Determination of lignin content

The method referred to Sluiter et al. (2010). The dried and weighed sample was placed in a taring pressure tube. Firstly, 72% sulfuric acid was added to poplar samples in the tube, and hydrolysis was carried out for 60 min in a water bath at 30 ± 2 °C, in which the mixture of the sulfuric acid and poplar samples was well mixed by stirring. Thereafter, the test tube was taken out and deionized water was added to dilute the acid to a concentration of 4% and placed in a high temperature sterilizer at 121 ± 2 °C for 1 h. When the reaction was completed, the solution was separated by filtration. After diluting the supernatant, the content of acid-soluble lignin was measured to be 205 nm using an ultraviolet spectrophotometer (UV-1800). The residue was placed in a 105 ± 2 °C oven and weighed constantly, and then placed in a muffle furnace at 575 ± 2 °C. The organic matter was pyrolyzed at a high temperature, and after 3 h of reaction, the sample was cooled and weighed again. The weight difference between before and after treatment was the acid insoluble lignin content.

Pretreatment for N₂ adsorption measurement

Five finished delignified samples were separately ground using the RHP-400 high-speed multi-function

grinding machine (RONGHAO, Chain) and passed through a 150-mesh screen. The weight of each sample was approximately 1.5 g. The water in each sample was replaced with ethanol (i.e., dehydrated) and subjected to successive 30%, 50%, 70%, 90%, 100%, 100%, and 100% gradient dehydration displacements with ethanol. The dehydrated sample was then subjected to the next degassing treatment. The K850 model critical point dryer (CPD) manufactured by British EMITECH was used to dry samples at a liquid carbon dioxide temperature for more than 8 h. This procedure ran under the temperature of around -3 to 42 °C. The supercritical drying method is currently the most suitable drying method for nitrogen adsorption measurement. By controlling the pressure and temperature to reach the critical point of the material, the sample without structural damages can be obtained, which was more accurate and reliable in the adsorption measurement (Chang et al 2011b).

N₂ adsorption measurement

The pretreated samples were tested using the ASAP2020 HD88 fully automated specific surface area and pore size profiler (Micromeritics, USA). It should be noted that, in order to ensure not be contaminated, the sample must be stored and tested in a test tube as soon as it is removed from the supercritical dryer. It is best to operate in a low temperature carbon dioxide environment to avoid the prolonged exposure in air. The sample was tested for adsorption of nitrogen molecules in the instrument at the liquid nitrogen temperature of 77 K, isothermal adsorption, desorption line was drawn, and more sample information was obtained by the further analysis. The entire test process lasted approximately 8 h.

BET and BJH method

Many characterization methods can be used to examine various ultrastructural properties of wood material (Wang et al. 2018a). In order to study the effect of the delignification on the pore structure of poplar cell wall, the N₂ adsorption volume, specific surface area, pore volume and mesoporous distribution of the progressive delignification treatment of poplar were examined by the N₂ adsorption method. The BET and BJH (Brunauer–Emmett–Teller) model were

respectively used to investigate the surface area and the pore size distribution of the mesopores during the lignin removal process in this study.

The BET theory (Quirk 1955) is based on the multi-molecular-layer adsorption model, and derives the relationship equation between the single-layer adsorption amount V_m and the multi-layer adsorption amount V , which is the BET equation as shown in Eq. (1):

$$\frac{P}{V_{ads}(P_0 - P)} = \frac{1}{V_m C} + \frac{C - 1}{V_m C} \left(\frac{P}{P_0} \right) \quad (1)$$

where P : nitrogen partial pressure; P_0 : saturation vapor pressure; V : amount of vapor adsorbed at P ; V_m : quantity of adsorbate forming a monolayer; C : constant related to sample adsorption capacity.

The model of pore size analysis used the principle of capillary condensation and volume equivalent substitution, where the Kelvin equation was basic for calculating the aperture. The BJH (Barrett–Joiner–Halenda) pore size distribution calculation model used the cylindrical model, which is a widely used mesoporous analysis method. This model simplified the shape of the hole and was confirmed that the analysis results were highly efficient and reliable (Kimura et al. 2016). Here is the BJH Eq. (2):

$$V_n = R_n \Delta V_n - R_n \Delta t_n \sum_{j=1}^{n-1} c_j A_p \quad (2)$$

where V_n : the volume of the pores involved in the n th desorption step; R_n , c_j : constants related to the average pore size and average thickness of the physically adsorbed multilayer; Δt_n : decrease in thickness of the multilayer; A_p : the area of each pore, from $A_p = 2V_p/r_p$ (Barrett et al. 1951; Masthan et al. 1992).

In many cases, in order to show the pore size distributions clearer, derivation will be performed, such as dV/dD .

Result and discussion

Examination of conditions

In order to determine the appropriate treatment time to achieve the desired delignification percentages, a preliminary experiment was performed. It was hoped that the experimental conditions would be determined by this empirical method. In the first pre-experiment,

the delignification treatment time of the samples was set to be 0, 2, 4, ..., 32, or 34 h, and the lignin content was measured. Lignin concentrations were tested using a two-step acid hydrolysis according to the method of Sluiter et al. (2010).

The delignification results are shown in Table 1. During the preliminary experiment, the interval between each treatment initially was set to 2 h. However, it was found that the removal amount of lignin between 0 and 2 h was too large, resulting in some useful information loss possibly. Therefore, the treatment of delignification for 1 h was added between 0 and 2 h. Finally, treatment times of 0, 1, 6, 10 and 32 h were selected as samples in this study. Moreover, named these five samples from Del-1 to Del-5 according to 0, 1, 6, 10 and 32 h treatment, respectively. The 25% span selected here was moderate as a gradient between samples.

Table 1 only shows the data of lignin, because it was the emphasis in this study. Besides that, during the delignification, the hemicellulose reduced by 9%, and cellulose content remained unchanged.

Table 1 Delignification under different treatment times

Treatment time (h)	Lignin (%)	Delignification degree (%)
0	27.3	0
1	22.6	22.0
2	18.7	31.4
4	16.5	39.7
6	14.8	45.8
8	9.1	66.6
10	5.6	79.6
12	3.2	88.3
14	3.2	88.4
16	3.1	88.8
18	2.9	89.3
20	2.6	90.7
22	2.5	90.9
24	1.9	92.9
28	1.6	94.2
32	1.4	94.9
34	0.2	99.4

Delignification degree = $1 - (\text{current lignin/lignin of untreated sample}) \times 100\%$

N₂ adsorption isotherm

As shown in Fig. 1, with the decrease of lignin residue, the adsorption amount of N₂ in the sample obviously increased, and the maximum adsorption volume also basically increased. This finding was confirmed in most delignified wood species (Kimura et al 2014, 2016). When five samples were sorted into two groups, i.e., Del-1 and Del-2 as the first one and Del-3 to Del-5 as the second one, it was found that the maximum adsorption capacity of the second one was prominent higher than the first one. Moreover, the internal data of each group were relatively close, and stable at 3.8 and 5–6 cm³ g⁻¹, respectively. It was indicated that, in the range of 25–50% of delignification, the N₂ adsorption capacity of poplar was changed in a larger degree. In addition, during the adsorption measurement, the amount of adsorption in the previous stage of Del-1 to Del-4 was small, and there was no prominent increase. Basically, a large adsorption volume occurred at the relative pressure $P/P_0 \approx 0.8$. It was illustrated that there were more mesopores in the samples than micropores. However, the growth of the isotherms of the Del-5 samples was relatively flat, and the first four samples had a distinct hysteresis loop. According to the classification from International Union of Pure and Applied Chemistry (IUPAC), the hysteresis loop was similar to the H₂ type (Sing 1985). The shape of the hole can be analyzed based on the type of the hysteresis loop. The hysteresis loop refers to the loop formed in the isotherm between the

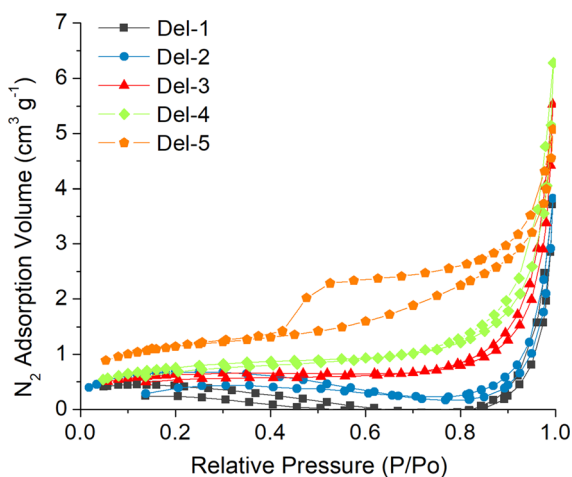


Fig. 1 Adsorption and desorption isotherms of Del-1 to Del-5 samples

adsorption and desorption lines. Actually, the cause of the H₂ type is complicated, and the shape can be simplified to a narrow ink bottle shape in general (Groen and Pérez-Ramírez 2004).

To evaluate the effect of different treatment time durations (Del-1 to Del-5), the Duncan's multiple range test (Duncan 1955) was utilized for the multiple comparison as shown in Table 2. According to the measurement of the BET specific surface area, the specific surface area of the five samples basically kept increasing. In particular, the Del-5 sample of 95% delignification achieved the highest value of 3.78 m² g⁻¹, which was three times as much as the untreated sample. Del-1 to Del-2 and Del-4 to Del-5 had larger changes in specific surface area, which can be proved by the statistical differences in Table 2. And it can be seen that the removal of lignin between these two spans increased more pores. This finding was also consistent with the results of previous reports.

Therefore, the amount of N₂ adsorption increased with the delignification, but their relationship was nonlinear, and there was a big gap between 25 and 50% of delignification. The specific surface area increased as the lignin content decreased.

As shown in Table 3, many studies on wood cell walls were completed. The structure of the microscopic pores can be explored according to different treatment methods including delignification, heat treatment, and different parts of the wood. Although the treatment methods were different, it was still related to the chemical composition of wood, especially the lignin. Therefore, delignification was the most direct method. Among them, the progressive delignification was a relative convincing treatment method, and it was generally to control the number of treatments or directly control the lignin content. Nakatani et al. (2008) and Kimura et al. (2014) used the number of delignification treatments, that pointed out micropores were present in lignin and 4–5 nm mesopores were concentrated. In addition, Stone and Scallan (1965) directly controlled the degree of delignification, and concluded that the 2–10 and 2–4 nm pores appeared were also consistent. Moreover, the detailed lignin content of this study was more quantitative and accurate. The whole process of pore change was also explored by the processive delignification. The relationship between lignin and pore structure was further improved.

Table 2 Experimental and statistical analysis results of mesopore structure of cell wall with different delignification times

Name	Processing time (h)	Degree of delignification (%)	N ₂ maximum adsorption volume (cm ³ g ⁻¹)	BET surface area (m ² g ⁻¹)	BJH pore volume (cm ³ g ⁻¹)	BJH Adsorption average pore diameter (nm)	Pore diameter at distribution peaks (nm)
Del-1	0	0 (0)a	3.7154 (0.0528)a	1.0246 (0.0144)a	0.005709 (0.000,278)a	55.0359 (2.8681)a	17.35 (0.73)a
Del-2	1	21.88 (1.12)b	3.8068 (0.0608)b	2.0855 (0.1498)b	0.005361 (0.000416)a	33.5433 (2.6590)b	7.28 (1.36)b
Del-3	6	45.24 (1.65)c	5.5879 (0.9251)c	2.0351 (0.1740)b	0.008064 (0.000143)b	35.0895 (1.7369)b	11.47 (1.95)c
Del-4	10	79.36 (1.38)d	6.2522 (0.5898)d	2.5282 (0.3291)c	0.009302 (0.000218)c	22.6558 (2.1954)c	2.56 (0.66)d
Del-5	32	94.43 (1.66)e	5.0663 (0.4836)e	3.7824 (0.6685)d	0.007076 (0.000347)d	12.4545 (1.4216)d	2.22 (0.38)d

Groups with the same letters in each column indicate that there is no statistical difference ($p < 0.05$) between the samples according to the Duncan's multiple range test
Values in parentheses are standard deviations

Table 3 Summary and comparison of wood cell wall pore research results

Classification	Study	Wood species	Treatment	Status and size	Conclusion
Progressive delignification	This study	Hybrid poplar	Progressive delignification (different delignification percentage)	Powders (150 mesh)	Delignification caused mesopores in 2–10 nm. The delignification process can be divided into initial, transitional and stable phase
	Stone and Scallan (1965)	Black spruce wood (<i>Picea marianu</i>)	Progressive delignification (different delignification percentage)	Powders (40–60 mesh); long fiber fraction (28–48 mesh)	Delignification produced 2–4 nm pores in the cell wall
	Nakatani et al. (2008)	Japanese cypress (<i>Chamaecyparis obtusa</i>)	Progressive delignification (different number of delignification treatments)	Powders (60–83 mesh)	Micropores (< 0.6 nm) decrease as lignin residues decrease, which presented in lignin
	Kimura et al. (2014)	North American Douglas fir (<i>Pseudotsuga menziesii</i>)	Progressive delignification (different number of delignification treatments)	Powders	Regardless of the degree of delignification, the mesopore diameter is 4–5 nm
Heat treatment	Nakatani et al. (2008)	Conifer pulp	Air drying	Cellulose	Micropores were scarce
	Kojiro et al. (2010)	Himoki (<i>Chamaecyparis obtusa</i> Endl.), Buna (<i>Fagus crenata</i> Bl.)	Heat treatment (50–160 °C)	Cubes (edge length \leq 2 mm)	Micropores were related to lignin concentration; heating caused a large decrease in micropores and no big change in mesopores
Part and properties	Kimura et al. (2016)	Softwood bleached kraft pulps (mixed softwoods); Hardwood bleached kraft pulps (<i>Eucalyptus globulus</i>)	Heat-drying and re-wetting treatment	Fines-free pulps (150 mesh)	Never-dried SBKP and HBKP pore sizes were concentrated at 8–10 nm; HBKP pore size peak was smaller than SBKP, which is related to lignin content
	Monteiro (2018)	Poplar (<i>genus populus</i>)	No treatment; Heat treatment (250, 300, 350, 400, 450 and 500 °C)	Powders (0.63 mm of diameter)	25 nm pores were formed at 250–400 °C; pore volume of 40–50 nm raised and then dropped
	Chang et al. (2009)	Six tropical rainforest species	Tension and normal wood	Sticks (5 mm \times 131 mm ²)	Mesoporosity increases with the thickness of the G-layer
	Chang et al. (2015)	Poplar (<i>Populus deltoides</i> \times <i>P. nigra</i>)	Tension wood and opposite wood	Cubes	Mesoporous volume decreased after deposition of G-layer
Others	Yin et al. (2015)	Chinese fir (<i>Cunninghamia lanceolata</i>)	Sapwood and heartwood	Cubes [10 mm (L) \times 4 mm (R) \times 10 mm (T)]	More mesopores in sapwood; more micropores in heartwood
	Shi and Avramidis (2018)	Western red cedar (<i>Thuja plicata</i>)	No extracted; extracted	Powders (20 mesh)	The pores of 10–36 nm belonged to the pit membrane; the extractives affected the distribution of micropores from 0.4–0.6 nm

In addition, the heat treatment test also confirmed the relationship between lignin and pore structure. During the heat treatment, especially at lower temperatures, the chemical composition of the lignin was not altered. However, micropores were greatly reduced due to moisture and other physical changes (Nakatani et al. 2008; Kojiro et al. 2010). For pulp, pores mostly appeared within 10 nm and the pore size was slightly different due to the lignin concentration (Kimura et al. 2016). However, the higher heat treatment temperatures resulted in larger mesopores, and pores above 25 nm were rarely seen in other treatments (Monteiro 2018). The changes brought about by the drying process were reversible, but only indicated the existence of relationship between lignin and pore structure, without further explanation. The different pore structures of different parts of wood were also related to the lignin content. The pore structures of G-layer in the heartwood and sapwood were consistent with other research results due to the chemical composition. Studies on extracts have also been shown to be associated with micropores (Shi and Avramidis 2018).

BJH pore size distribution and pore volume

The available aperture range of the BJH model was approximately 1.7–300 nm. That was more suitable for mesopores, so the accuracy in 2–50 nm range was higher, which was the research object of this study. The portion smaller than 2 nm was only selected from the data point closest to 2 nm, which had the pore diameters of 1.97–2 nm. This can better reflect the characteristics of the change process while ensuring accuracy.

As shown in Table 2, the BJH mesoporous pore volume of Del-2 to Del-4 was significantly increased and was consistent with the variation of the maximum adsorption volume of N_2 . This was because the assumption of N_2 adsorption was to some extent the pore volume. The pore volume directly expressed the total volume of the pores, but did not completely reflect the number of mesopores because the morphology and depth of the different pores were unknown.

In Fig. 2, the untreated Del-1 sample contained almost no pores of 10 nm or smaller, and the mesopores were only distributed at 10–50 nm. The mesopores with 2–10 nm pore size appeared after the

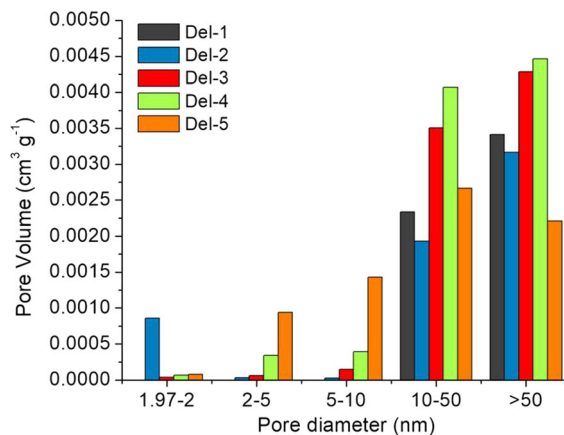


Fig. 2 Sample pore volume distribution under different pore sizes

delignification, and pore volume of the pores in this range increased rapidly with the decrease of lignin content. The pore volume of Del-5 at 2–5 nm and 5–10 nm reached $0.000939 \text{ cm}^3 \text{ g}^{-1}$ and $0.001431 \text{ cm}^3 \text{ g}^{-1}$, respectively, and the sum of the two accounted for one-third of the total pore volume. There was also a study reporting that the 50 nm pore volume of 100% lignin removal sample was smaller than that of 80% lignin removal sample (Stone and Scallan 1965). Also, based on that, another explanation was proposed. It might be because some hemicellulose degraded and fell into the large pores (> 50 nm). These decomposition components filled the large pores and reduced their diameters. Therefore, the final result was that the pore volume of Del-5 at 50 nm was rather reduced.

The pore volume distribution of the five samples was similar in the 10–50 nm and > 50 nm intervals. There were two reasons for the decrease of Del-2 pore volume:

1. the formation of new pores on the cell wall, which caused a large number of pores around 2 nm;
2. the removal of lignin to enlarge the original pores.

For the first hypothesis, the part of the wood cell wall that was originally filled with lignin formed a new hole due to the delignification treatment. This was related to the lignin content and distribution of the cell wall, and the surface layer and the high lignin concentration may be more effective, such as in the

high-lignin composites, compound middle lamella and the cell corners (Fromm et al. 2003).

Moreover, it can be assumed that two variables, the amount of lignin removed and the pore size, were proportional. So that the pores of the original pore size in the pores of 10 to 50 nm were expanded to 50 nm or larger, and the pores of > 50 nm became larger and beyond the test range. The treatment of Del-3 and Del-4 then allowed the pore volume in these two intervals to increase further. Finally, the lignin content of the Del-5 sample was extremely low, and the pores were basically composed of cellulose and hemicellulose after the influence of lignin was excluded.

As seen in Table 2, the average pore size of the BJH mesopores was decreased, which was contrary to the pre-test before the experiment. Why did the pores increase but the average pore size decreases? Because the number of holes formed in different pore size ranges was inconsistent. Obviously, the smaller mesoporous pore volume of 2–10 nm grew faster.

Therefore, with the delignification, the pore volume of 2–10 nm pore size continued to grow rapidly, which was consistent with the result of 2–4 nm pores after the removal of black spruce (Stone and Scallan 1965). Most pores in the pulp belonged to mesopores of 10 nm and larger, as shown in Table 3 (Stone and Scallan 1968; Scallan 1978; Alince and Van de Ven 1997). The pores of 10–50 nm and larger increased but decreased at the end. In general, the delignification caused a large number of mesopores in the wood cell wall, mainly concentrated in the 2–10 nm pore diameter range, and the average pore size decreased during the delignification.

Pore size distributions

Figure 3 demonstrates the pore size distributions of all samples, in which, the pore volume/pore diameter (dV/dD) is the vertical ordinate, and the pore diameter (D) is the horizontal ordinate. The direct meaning of the ordinate was the rate of change of the aperture, which can visually display the pore size distribution. The first point of the x -axis in the figure is 1.97 nm, which is slightly smaller than 2 nm.

From the curve shape of Del-2 to Del-5, it can be seen that the amount of micropores at 1.9–2 nm was extremely large, which was several times of the mesoporous value. The second curve had a unique peak at 5–15 nm, then the number cut back. Del-1 had

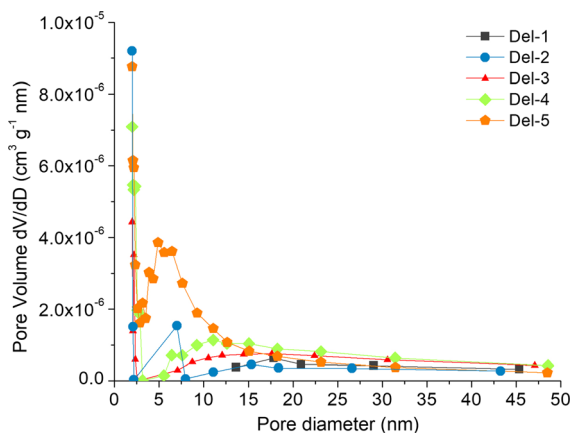


Fig. 3 BJH pore size distributions of Del-1 to Del-5 samples

different behaviors, since its data appeared after 10 nm and there was no micropores of 1.9–2 nm. However, after that it had the characteristics of the unique peak and the shape of the curve was consistent with other samples. The delignificated poplar would have a large number of 1.98–10 nm pores, meaning that the surface lignin was detached and the mesopores were exposed.

In general, the low lignin concentration corresponded to a smaller pore size peak, and studies have certified that eucalyptus pulp (HBKP) had a smaller pore diameter than mixed softwood pulp (SBKP) during pulping (Kimura et al 2016), and hardwood also contained more micropores (Kojiro et al 2010). The peak analysis of the five samples in this study found that Del-2 had a special curve, and the peaks of the other four samples continued to move to the left and upward. Firstly, the changes of Del-1, 3, 4, and 5 samples were that, as the degree of delignification increased, the pore sizes corresponding to the peaks of Del-1, 3, 4, and 5 samples were 17.35, 11.47, 2.56 and 2.22 nm, respectively, and the pore size was steadily decreased. The height value of the peak also had a clear upward trend, indicating that the number of pores in the cell wall was larger and the concentration became higher. The width of the peak turned to smaller, namely, narrower, and it was shown that the uniformity of the pores became higher.

Followed by the Del-2 curve, its overall characteristics were consistent with other samples, but its unnormal high peak reflected to the smaller aperture and larger quantity, which were clearly different from the trends of Del-1, 3, 4, and 5 samples. In this aspect,

this study revealed that the reason was that the Del-2 sample was in the primary stage of delignification, and the internal structure was not shaped, so a mutation appears during the delignification process. Compared with the Del-1 sample, the biggest change of the Del-2 sample was that the pores with smaller pore sizes (1.9–2.1 nm and about 7 nm) appeared in large quantities, so its maximum adsorption volume of N_2 was not much changed but the specific surface area was obviously increased. It was further speculated that this part of the pore may be the one of the sources of pores at the peaks of the Del-2 to 5 samples. Thereafter, as the delignification treatment continued, the sample settled to the Del-2 phase, and the change of Del-2 to 5 was carried out within the shaped pore structure.

Therefore, the delignification reduced the pore size of the poplar cell wall pores, and finally formed a large number of uniform pores of about 2.1 nm. The change process did not happen completely smoothly, but with a mutation at 25% delignification.

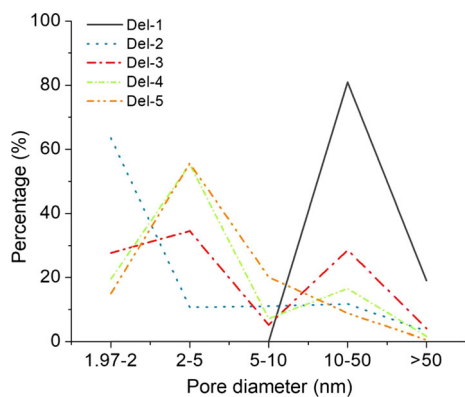


Fig. 4 Pore size distribution ratio

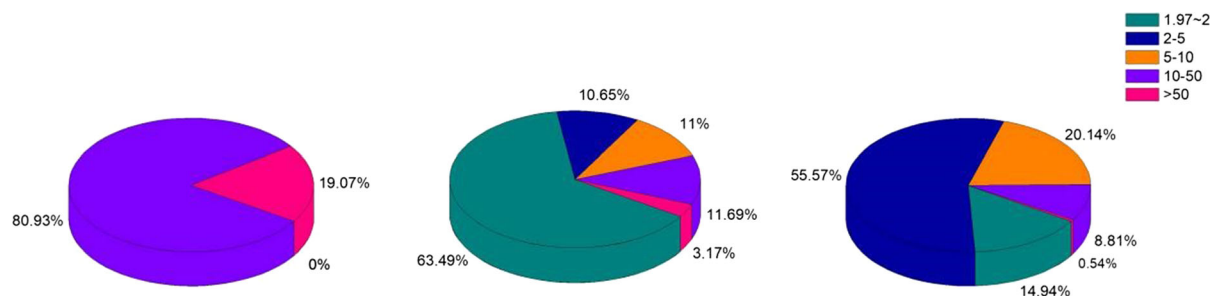


Fig. 5 Del-1, Del-2, Del-5 pore size distribution pie chart

By classifying the pore size distributions, the percentage of each pore size interval of the sample was obtained and is shown in Fig. 4. It can still be found that the poplar cell wall pore structure changed from Del-1 (initial phase) to Del-2 (transitional phase) during the delignification and was shaped in Del-3, 4, 5 (stable phase). There was a clear difference among the three phases, while the distribution ratios and trends of Del-3, 4, and 5 in the same stable phase were consistent. Figure 5 shows the most representative three samples, Del-1, Del-2 and Del-5, in every phase. From which, it was clearly revealed that the main pore diameters of the three phases were 10–50 nm, 1.9–2 nm and 2–5 nm, respectively.

Conclusions

The results obtained were concluded as follows:

1. Delignification increased the N_2 adsorption volume and specific surface area of poplar. These two were not completely linear relation with the delignification degree, and the increase in some intervals was uneven.
2. Delignification caused a mass of mesopores in the cell wall, mainly concentrated in the 2 to 10 nm pore size range, and the average pore diameter decreased as the progress of the delignification.
3. The whole delignification process can be roughly divided into three phases, i.e., initial phase, transitional phase and stable phase, with pore sizes of 10–50 nm, 1.9–2 nm and 2–5 nm, respectively. The change of process was not completely uniform. After the three phases, the pore size of the poplar cell wall pores was reduced, and finally a good deal of uniform pores about 2.1 nm were formed.

Acknowledgments The authors are thankful for financial support from the National Strategic Research and Development Program of China (2017YFD0600202), and the National Natural Science Foundation of China (31670558).

Compliance with ethical standards

Conflict of interest All authors declare that they have no conflict of interest.

References

- Akitomo M, Suzuki R, Ishimaru Y, Iida I, Furuta Y (2006) Micropore structure of wood and bamboo charcoals: establishment of a method for the calculation of effective pore size distribution and the possibility of controlling micropore structure. *Jpn Wood Res Soc (Jpn)* 56:107–111
- Alince B, Van de Ven TGM (1997) Porosity of swollen pulp fibers evaluated by polymer adsorption. *Fundam Papermak Mater* 2:771–788
- Barrett EP, Joyner LG, Halenda PP (1951) The determination of pore volume and area distributions in porous substances. I. Computations from nitrogen isotherms. *J Am Chem Soc* 73(1):373–380
- Basso MC, Cerrella EG, Cukierman AL (2005) Cadmium uptake by lignocellulosic materials: effect of lignin content. *Sep Sci Technol* 39(5):1163–1175
- Borrega M, Kärenlampi PP (2011) Cell wall porosity in Norway spruce wood as affected by high-temperature drying. *Wood Fiber Sci* 43(2):206–214
- Brunauer S, Emmett PH, Teller E (1938) Adsorption of gases in multimolecular layers. *J Am Chem Soc* 60(2):309–319
- Carrott PJM, Carrott MR (2007) Lignin—from natural adsorbent to activated carbon: a review. *Biores Technol* 98(12):2301–2312
- Chang SS, Clair B, Ruelle J, Beauchêne J, Di Renzo F, Quignard F, Gril J (2009) Mesoporosity as a new parameter for understanding tension stress generation in trees. *J Exp Bot* 60(11):3023–3030
- Chang SS, Hu J, Bruno C, Françoise Q (2011a) Pore structure characterization of poplar tension wood by nitrogen adsorption–desorption method. *Sci Silvae Sin* 47(10):134–140
- Chang S, Hu J, Zhao G (2011b) Effects of different drying pretreatments on pore structure of poplar tension wood. *J Beijing For Univ* 33(2):91–95
- Chang SS, Quignard F, Alméras T, Clair B (2015) Mesoporosity changes from cambium to mature tension wood: a new step toward the understanding of maturation stress generation in trees. *New Phytol* 205(3):1277–1287
- Dawson BS, Pearson H (2017) Effect of supercritical CO₂ dewatering followed by oven-drying of softwood and hardwood timbers. *Wood Sci Technol* 51(4):771–784
- Deshpande AS, Burgert I, Paris O (2006) Hierarchically structured ceramics by high-precision nanoparticle casting of wood. *Small* 2(8–9):994–998
- Dietrich D, Lampke T, Rößler R (2013) A microstructure study on silicified wood from the Permian Petrified Forest of Chemnitz. *Paläontol Z* 87(3):397–407
- Dietrich D, Viney M, Lampke T (2015) Petrifications and wood-templated ceramics: comparisons between natural and artificial silicification. *IAWA J* 36(2):167–185
- Dizhbite T, Zakis G, Kizima A, Lazareva E, Rossinskaya G, Jurkane V, Viesturs U (1999) Lignin—a useful biore-source for the production of sorption-active materials. *Biores Technol* 67(3):221–228
- Donaldson LA, Cairns M, Hill SJ (2018) Comparison of micropore distribution in cell walls of softwood and hardwood xylem. *Plant Physiol* 178(3):1142–1153
- Duncan DB (1955) Multiple range and multiple *F* tests. *Biometrics* 11(1):1–42
- Fahlén J, Salmén L (2005) Pore and matrix distribution in the fiber wall revealed by atomic force microscopy and image analysis. *Biomacromol* 6(1):433–438
- Fink S (1992) Transparent wood—a new approach in the functional study of wood structure. *Holzforsch Int J Biol Chem Phys Technol Wood* 46(5):403–408
- Franklin GL (1945) Preparation of thin sections of synthetic resins and wood–resin composites, and a new macerating method for wood. *Nature* 155(3924):51
- Fromm J, Rockel B, Lautner S, Windeisen E, Wanner G (2003) Lignin distribution in wood cell walls determined by TEM and backscattered SEM techniques. *J Struct Biol* 143(1):77–84
- Galarneau A, Desplandier D, Dutartre R, Di Renzo F (1999) Micelle-templated silicates as a test bed for methods of mesopore size evaluation. *Microporous Mesoporous Mater* 27(2–3):297–308
- Groen JC, Pérez-Ramírez J (2004) Critical appraisal of mesopore characterization by adsorption analysis. *Appl Catal A General* 268(1–2):121–125
- He Y, Li Z, Xi H, Guo J, Xia Q (2004) Research progress of gas–solid adsorption isotherms. *Ion Exch Adsorpt* 20:376–384
- Innes WB (1957) Use of parallel plate model in calculation of pore size distribution. *Anal Chem* 29(7):1069–1073
- Ishizawa CI, Davis MF, Schell DF, Johnson DK (2007) Porosity and its effect on the digestibility of dilute sulfuric acid pretreated corn stover. *J Agric Food Chem* 55(7):2575–2581
- Kimura M, Qi ZD, Fukuzumi H, Kuga S, Isogai A (2014) Mesoporous structures in never-dried softwood cellulose fibers investigated by nitrogen adsorption. *Cellulose* 21(5):3193–3201
- Kimura M, Qi ZD, Isogai A (2016) Analysis of mesopore structures in wood cell walls and pulp fibers by nitrogen adsorption method. *Nord Pulp Pap Res J* 31(2):198–204
- Kojiro K, Furuta Y, Ishimaru Y (2008) Influence of heating and drying history on micropores in dry wood. *J Wood Sci* 54(3):202–207
- Kojiro K, Miki T, Sugimoto H, Nakajima M, Kanayama K (2010) Micropores and mesopores in the cell wall of dry wood. *J Wood Sci* 56(2):107–111
- Masthan SK, Rao KR, Prasad PS, Rao PK (1992) Derivation of the expanded form of the BJH equation and its application to the pore structure analysis of mesoporous adsorbents. *Adsorpt Sci Technol* 9(4):212–230
- Meng X, Foston M, Leisen J, DeMartini J, Wyman CE, Ragauskas AJ (2013) Determination of porosity of lignocellulosic biomass before and after pretreatment by using

- Simons' stain and NMR techniques. *Biores Technol* 144:467–476
- Meng X, Wells T, Sun Q, Huang F, Ragauskas A (2015) Insights into the effect of dilute acid, hot water or alkaline pre-treatment on the cellulose accessible surface area and the overall porosity of *Populus*. *Green Chem* 17(8):4239–4246
- Mizutani M, Takase H, Adachi N, Ota T, Daimon K, Hikichi Y (2005) Porous ceramics prepared by mimicking silicified wood. *Sci Technol Adv Mater* 6(1):76
- Monteiro G (2018) Structural characterization of heat treated poplar wood. *U Porto J Eng* 4(1):9–26
- Nakatani T, Ishimaru Y, Iida I, Furuta Y (2008) Micropore structure of wood: change in micropore structure accompanied by delignification. *J Wood Sci* 54(3):252–255
- Persson PV, Fogden A, Hafrén J, Daniel G, Iversen T (2004a) Silica-cast replicas for morphology studies on spruce and birch xylem. *IAWA J* 25(2):155–164
- Persson PV, Hafrén J, Fogden A, Daniel G, Iversen T (2004b) Silica nanocasts of wood fibers: a study of cell-wall accessibility and structure. *Biomacromol* 5(3):1097–1101
- Quirk JP (1955) Significance of surface areas calculated from water vapor sorption isotherms by use of the BET equation. *Soil Sci* 80(6):423–430
- Rouquerol J, Rouquerol F, Llewellyn P, Maurin G, Sing KS (2013) Adsorption by powders and porous solids: principles, methodology and applications. Academic Press, Berlin
- Ruelle J (2014) Morphology, anatomy and ultrastructure of reaction wood. In: Gardiner B, Barnett J, Saranpää P, Gril J (eds) *The biology of reaction wood*. Springer, Berlin, pp 13–35
- Sarkar P, Auer M (2017) Organization of the plant cell wall. *Mol Cell Biol Growth Differ Plant Cells* 101:1550–1568
- Scallan AM (1978) Fibre-water interactions in paper-making. *Trans Symp Oxford* 1:9–27
- Shi J, Avramidis S (2018) Dried cell wall nanopore configuration of Douglas-fir, western red cedar and aspen heartwoods. *Wood Sci Technol* 52(4):1025–1037
- Sing KS (1985) Reporting physisorption data for gas/solid systems with special reference to the determination of surface area and porosity. *Pure Appl Chem* 57(4):603–619
- Sluiter A, Hames B, Ruiz R, Scarlata C, Sluiter J, Templeton D, Crocker D (2010) Determination of structural carbohydrates and lignin in biomass. *Laboratory Analytical Procedure (TP-510-42618)*
- Stone JE (1964) The porous structure of wood and fibres. *Pulp Pap Mag Can* 65(1):T3–T13
- Stone JE, Scallan AM (1965) Effect of component removal upon the porous structure of the cell wall of wood. *J Polym Sci C Polym Symp* 11(1):13–25
- Stone JE, Scallan AM (1968) The effect of component removal upon the porous structure of the cell wall of wood. Part III. A comparison between the sulphite and kraft processes. *Pulp Pap Mag Can* 6:69–74
- Wang X, Liu Z, Zhang Y, Pan B (2018a) Characterization methods of wood ultrastructure and its research progress. *Chem Ind Prod* 38(2):1–10
- Wang X, Zhan T, Liu Y, Shi J, Pan B, Zhang Y, Shi SQ (2018b) Large-size transparent wood for energy-saving building applications. *ChemSusChem* 11(23):4086–4093
- Wu J, Wu Y, Yang F, Tang C, Huang Q, Zhang J (2019) Impact of delignification on morphological, optical and mechanical properties of transparent wood. *Compos A Appl Sci Manuf Appl Sci Manuf* 117:324–331
- Yin J, Song K, Lu Y, Zhao G, Yin Y (2015) Comparison of changes in micropores and mesopores in the wood cell walls of sapwood and heartwood. *Wood Sci Technol* 49(5):987–1001
- Zhu M, Song J, Li T, Gong A, Wang Y, Dai J, Hu L (2016) Highly anisotropic, highly transparent wood composites. *Adv Mater* 28(26):5181–5187

Publisher's Note Springer Nature remains neutral with regard to jurisdictional claims in published maps and institutional affiliations.